ICES REPORT 10-40

October 2010

On Linear Independence of T-splines

by

X. Li, J. Zheng, T.W. Sederberg, T.J.R. Hughes, M.A. Scott

The Institute for Computational Engineering and Sciences
The University of Texas at Austin
Austin, Texas 78712

Reference: X. Li, J. Zheng, T.W. Sederberg, T.J.R. Hughes, M.A. Scott, "On Linear Independence of T-splines", ICES REPORT 10-40, The Institute for Computational Engineering and Sciences, The University of Texas at Austin, October 2010\.

On Linear Independence of T-splines

Xin Li[a], Jianmin Zheng[b], Thomas W. Sederberg[c,*], Thomas J. R. Hughes[d], Michael A. Scott[d]

[a] *University of Science and Technology of China, Hefei, Anhui, P. R. China*
[b] *School of Computer Engineering, Nanyang Technological University, Singapore*
[c] *Computer Science Department, Brigham Young University*
[d] *ICES, University of Texas at Austin*

Abstract

This paper shows that linear independence of any T-spline can be determined by computing the nullity of the T-spline-to-NURBS transform matrix, and that linear independence is therefore a function both of the control mesh topology and the knot values. The paper analyzes the class of T-splines for which no perpendicular T-junction extensions intersect, and shows that all such T-splines are linearly independent. The paper recommends such T-splines as being well-suited for isogeometric analysis.

Keywords: T-splines, linear independence, NURBS, isogeometric analysis

1. Introduction

T-splines (Sederberg et al., 2003, 2004) is a free-form geometric shape technology that solves many of the limitations inherent in the industry standard NURBS representation.

One advantage that T-splines have over NURBS is local refinement. While NURBS refinement requires the insertion of an entire row of control points, T-splines allow partial rows of control points that terminate in a special control point called a T-junction. Another advantage is that T-splines models are watertight, whereas NURBS models are typically comprised of many distinct patches that do not generally fit together without gaps. In particular, most trimmed NURBS models have mathematically unavoidable gaps which can be completely closed using an extension to T-splines (Sederberg

*tom@cs.byu.edu

et al., 2008). T-splines are forward and backward compatible with NURBS surfaces, and thus integrate well into existing CAD systems.

These capabilities that make T-splines attractive for use in CAD have also made T-splines desirable for use in isogeometric analysis (Bazilevs et al., 2010; Cottrell et al., 2009). Local refinement is valuable in analysis because it enables much smaller linear systems than would a similar NURBS solution. Watertightness is valuable because models that are not watertight often require substantial preprocessing to close the unwanted gaps, and in the process the "isogeometric" principle of using the identical model for CAD and analysis is violated. NURBS compatibility is valuable because NURBS is an industry standard CAD representation and widespread industrial adoption of isogeometric analysis will occur most easily with technologies that are compatible with existing standards.

A property of T-splines that has not been studied until recently is linear independence. While linear independence is not required (although it is desirable) for most CAGD applications, it is imperative for isogeometric analysis. Unfortunately, Buffa et al. (2010) gives an example of a linearly dependent T-spline surface, raising concerns that T-splines in its full generality may not be suitable for use in isogeometric analysis. Buffa et al. (2010) also presents a constructive method for devising a class of T-meshes that are linearly independent. However, not all linearly independent T-meshes can be obtained in this manner, and it is not obvious how to use the method to check whether a given T-mesh can be constructed using the method.

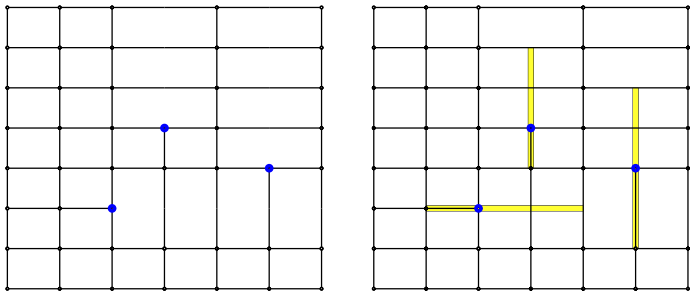

(a) Simple T-mesh. (b) T-junction extensions.

Figure 1: T-junction extensions on a simple T-mesh.

This paper presents a necessary and sufficient condition for a T-spline

surface to be linearly independent: if the nullity of the T-spline-to-NURBS transformation matrix is zero, the T-spline is linearly independent; otherwise, the T-spline is linearly dependent. This rather complicated condition is algebraic in nature, and is a function of T-mesh topology and of knot values. Using this condition, the paper identifies a class of T-splines that is always linearly independent, regardless of knot values. The class of T-splines is characterized by the simple topology requirement that no horizontal T-junction extension is allowed to intersect any vertical T-junction extension. T-junction extensions are illustrated in Figure 1, and described in detail in Section 6. In addition to having guaranteed linear independence, local refinement in such T-splines is well contained (Scott et al., 2010). Also, if some minor additional topological conditions are met at the boundaries of a non-periodic T-mesh, the polynomial basis functions for T-splines in this class sum identically to one (Li et al., 2010). For these reasons, we will refer in this paper to T-splines whose T-junction extensions do not intersect as *analysis-suitable T-splines*.

This paper is structured as follows. Pertinent background on T-splines is reviewed in Section 2. Section 3 discusses how to construct a matrix M that maps T-spline control points to the control points of an equivalent NURBS surface. Section 4 proves that M being full rank is a necessary and sufficient condition for the linear independence of a T-spline. Section 5 explains how T-mesh topology influences non-zero elements of M. This insight is used in Section 6 to prove that any analysis-suitable T-spline is linearly independent.

This paper is written specifically in terms of bicubic T-splines, although the concepts apply to any degree. T-splines of arbitrary degree are discussed in (Bazilevs et al., 2010; Finnigan, 2008).

2. Review of T-splines

Figure 2.a illustrates a T-mesh—a control grid for a T-spline surface (the equivalent NURBS in Figure 2.b is discussed in Section 3). Each vertical line segment is associated with an s_i knot value and each horizontal line segment is associated with a t_j knot value. The solid circles represent control points.

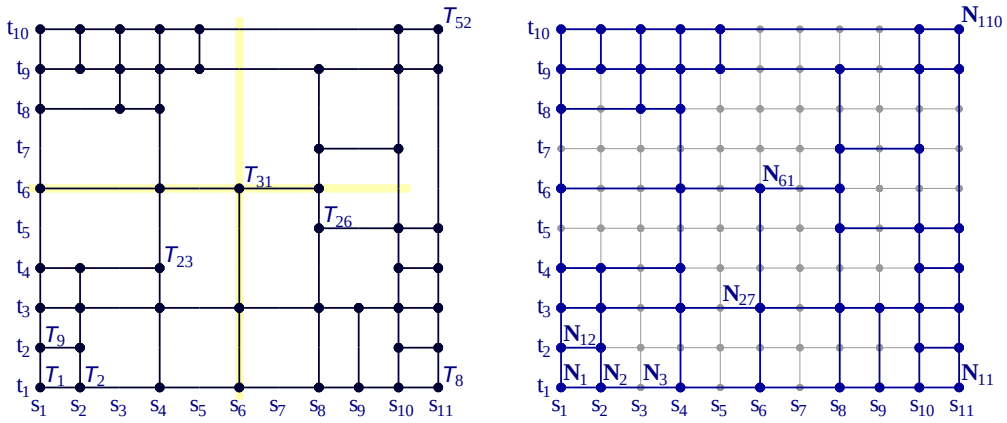

(a) T-mesh. (b) Underlying NURBS control mesh.

Figure 2: T-mesh diagram and the control mesh of the underlying NURBS.

The equation of a T-spline surface is given by:

$$\mathbf{T}(s,t) = \frac{\sum_{i=1}^{\tau} \mathbf{T}_i w_i T_i(s,t)}{\sum_{i=1}^{\tau} w_i T_i(s,t)} \tag{1}$$

or, in homogeneous form:

$$\mathcal{T}(s,t) = \sum_{i=1}^{\tau} (w_i \mathbf{T}_i, w_i)\, T_i(s,t) = \sum_{i=1}^{\tau} \mathcal{T}_i\, T_i(s,t) \tag{2}$$

where $\mathbf{T}_i = (x_i, y_i, z_i)$ are control points, w_i are weights, τ is the number of control points, and $\mathcal{T}_i = (w_i x_i, w_i y_i, w_i z_i, w_i)$ are homogeneous control points. The $T_i(s,t)$ in (1) and (2) are the T-spline basis functions[1] and are given by

$$T_i(s,t) = B[\vec{\mathbf{s}}_i](s) B[\vec{\mathbf{t}}_i](t) \tag{3}$$

[1]The term *basis function* implies linear independence. Since, as this paper shows, the vast majority of T-splines are linearly independent (including the one in Figure 2), we will refer to the $T_i(s,t)$ as basis functions, rather than the more generic term *blending functions*. In the case of a linearly dependent T-spline, it is more proper to speak of blending functions.

where $B[\vec{\mathbf{s}}_i](s)$ and $B[\vec{\mathbf{t}}_i](t)$ are the cubic B-spline basis functions associated with the knot vectors

$$\vec{\mathbf{s}}_i = [s_{\sigma_i^0}, s_{\sigma_i^1}, s_{\sigma_i^2}, s_{\sigma_i^3}, s_{\sigma_i^4}] \quad \text{and} \quad \vec{\mathbf{t}}_i = [t_{\tau_i^0}, t_{\tau_i^1}, t_{\tau_i^2}, t_{\tau_i^3}, t_{\tau_i^4}] \tag{4}$$

respectively. Each basis function is a piecewise polynomial given by

$$B[\vec{\mathbf{s}}_i](s) = \begin{cases} 0, & s \le s_{\sigma_i^0} \\ \frac{(s-s_{\sigma_i^0})^3}{(s_{\sigma_i^3}-s_{\sigma_i^0})(s_{\sigma_i^2}-s_{\sigma_i^0})(s_{\sigma_i^1}-s_{\sigma_i^0})}, & s_{\sigma_i^0} < s \le s_{\sigma_i^1} \\ \frac{(s-s_{\sigma_i^0})^2(s_{\sigma_i^2}-s)}{(s_{\sigma_i^3}-s_{\sigma_i^0})(s_{\sigma_i^2}-s_{\sigma_i^0})(s_{\sigma_i^2}-s_{\sigma_i^1})} + \frac{(s_{\sigma_i^3}-s)(s-s_{\sigma_i^1})(s-s_{\sigma_i^0})}{(s_{\sigma_i^2}-s_{\sigma_i^1})(s_{\sigma_i^3}-s_{\sigma_i^1})(s_{\sigma_i^3}-s_{\sigma_i^0})} + \\ \quad \frac{(s_{\sigma_i^4}-s)(s-s_{\sigma_i^1})^2}{(s_{\sigma_i^4}-s_{\sigma_i^1})(s_{\sigma_i^3}-s_{\sigma_i^1})(s_{\sigma_i^2}-s_{\sigma_i^1})}, & s_{\sigma_i^1} < s \le s_{\sigma_i^2} \\ \frac{(s-s_{\sigma_i^0})(s_{\sigma_i^3}-s)^2}{(s_{\sigma_i^3}-s_{\sigma_i^0})(s_{\sigma_i^3}-s_{\sigma_i^1})(s_{\sigma_i^3}-s_{\sigma_i^2})} + \frac{(s-s_{\sigma_i^1})(s_{\sigma_i^3}-s)(s_{\sigma_i^4}-s)}{(s_{\sigma_i^3}-s_{\sigma_i^2})(s_{\sigma_i^3}-s_{\sigma_i^1})(s_{\sigma_i^4}-s_{\sigma_i^1})} + \\ \quad \frac{(s_{\sigma_i^4}-s)^2(s-s_{\sigma_i^2})}{(s_{\sigma_i^4}-s_{\sigma_i^1})(s_{\sigma_i^4}-s_{\sigma_i^2})(s_{\sigma_i^3}-s_{\sigma_i^2})}, & s_{\sigma_i^2} < s \le s_{\sigma_i^3} \\ \frac{(s_{\sigma_i^4}-s)^3}{(s_{\sigma_i^4}-s_{\sigma_i^1})(s_{\sigma_i^4}-s_{\sigma_i^2})(s_{\sigma_i^4}-s_{\sigma_i^3})}, & s_{\sigma_i^3} < s \le s_{\sigma_i^4} \\ 0, & s_{\sigma_i^4} < s \end{cases} \tag{5}$$

The knot vectors $\vec{\mathbf{s}}_i$ and $\vec{\mathbf{t}}_i$ are inferred from the T-mesh (see Sederberg et al. (2003)). For example, $\vec{\mathbf{s}}_{31}$ for Figure 2.a consists of the five s-knot values of the vertical lines in the T-mesh intersected by the highlighted horizontal line, and likewise for $\vec{\mathbf{t}}_{31}$. Thus, $\vec{\mathbf{s}}_{31} = [s_1, s_4, s_6, s_8, s_{10}]$ and $\vec{\mathbf{t}}_{31} = [t_1, t_3, t_6, t_9, t_{10}]$. Likewise, $\vec{\mathbf{s}}_{23} = [s_1, s_2, s_4, s_6, s_8]$, $\vec{\mathbf{t}}_{23} = [t_1, t_3, t_4, t_6, t_8]$, $\vec{\mathbf{s}}_{26} = [s_4, s_6, s_8, s_{10}, s_{11}]$, and $\vec{\mathbf{t}}_{26} = [t_1, t_3, t_5, t_6, t_7]$. Once these knot vectors are determined for each basis function, the T-spline is defined using (1).

The *central knot indices* of a control point are the indices of the s and t knot lines that the pre-image of the control point lies on. Thus, the central knot indices for $\mathbf{T}_{31}$ in Figure 2 are $(6, 6)$ and the central knot indices for $\mathbf{T}_{26}$ are $(8, 5)$.

We will refer to $\vec{\mathbf{s}} = [s_{-1}, s_0, s_1, s_2, \ldots, s_c, s_{c+1}, s_{c+2}]$ and $\vec{\mathbf{t}} = [t_{-1}, t_0, t_1, t_2, \ldots t_r, t_{r+1}, t_{r+2}]$ as the *global knot vectors* for the T-spline. All $\vec{\mathbf{s}}_i$ are subsequences of $\vec{\mathbf{s}}$ and all $\vec{\mathbf{t}}_i$ are subsequences of $\vec{\mathbf{t}}$.

3. T-spline to NURBS conversion

The global knot vectors $\vec{\mathbf{s}}$ and $\vec{\mathbf{t}}$ can be used in defining a NURBS surface:

$$\mathbf{N}(s,t) = \frac{\sum_{j=1}^{c}\sum_{k=1}^{r} w_{jk}\mathbf{N}_{jk}N_{jk}(s,t)}{\sum_{j=1}^{c}\sum_{k=1}^{r} w_{jk}N_{jk}(s,t)} \tag{6}$$

where $\mathbf{N}_{jk}$ are control points, N_{jk} are basis functions, w_{jk} are weights, and r and c the are number of rows and columns in the control grid. In homogeneous form,

$$\mathcal{N}(s,t) = \sum_{j=1}^{c}\sum_{k=1}^{r} \mathcal{N}_{jk}N_{jk}(s,t) \tag{7}$$

where $\mathcal{N}_{jk}$ is the four-tuple $(w_{jk}\mathbf{N}_{jk}, w_{jk})$.

$$N_{jk}(s,t) = B_j(s)B_k(t) \tag{8}$$

where $B_j(s)$ and $B_k(t)$ are shorthand for

$$\begin{aligned} B_j(s) &= B[s_{j-2}, s_{j-1}, s_j, s_{j+1}, s_{j+2}](s), \\ B_k(t) &= B[t_{k-2}, t_{k-1}, t_k, t_{k+1}, t_{k+2}](t) \end{aligned} \tag{9}$$

as defined in (5), and the knots s_i and t_i belong to the global knot vectors. The central knot indices for N_{jk} are simply (j,k).

If $\mathcal{N}(s,t)$ and $\mathcal{T}(s,t)$ have the same global knot vectors, the $\mathcal{N}_{jk}$ can be uniquely determined such that $\mathcal{N}(s,t) \equiv \mathcal{T}(s,t)$. $\mathcal{N}(s,t)$ is called the *underlying NURBS* of $\mathcal{T}(s,t)$. Figure 2.b diagrams the underlying NURBS for the T-mesh in Figure 2.a. Conversion from T-spline to underlying NURBS plays a central role in this paper, so we now discuss it in detail.

Equations (6) and (7) use two subscripts to reference control points and basis functions. Conversion from T-spline to NURBS is more cleanly described using single subscript notation:

$$\mathcal{N}(s,t) = \sum_{k=1}^{\nu} \mathcal{N}_k \; N_k(s,t). \tag{10}$$

Each double-subscript pair in (7) maps to a unique single-subscripted variable in (10). We denote the map $k = \eta(i,j)$. In Figure 2.b, the single-subscripted

control points are listed in row-major order, so $\eta(i,j) = (j-1)c + i$. In this example, $\nu = 110$ and $\tau = 52$.

Each T-spline basis function is a linear combination of NURBS basis functions:

$$T_i(s,t) = \sum_{j=1}^{\nu} m_{j,i} N_j(s,t) \tag{11}$$

where the $m_{j,i}$ are found by knot insertion (see Section 3.1). Substituting (11) into (2),

$$\mathcal{T}(s,t) = \sum_{j=1}^{\tau} \mathcal{T}_j \left[\sum_{i=1}^{\nu} m_{i,j} N_i(s,t) \right] = \sum_{i=1}^{\nu} \left[\sum_{j=1}^{\tau} m_{i,j} \mathcal{T}_j \right] N_i(s,t) \tag{12}$$

which is equivalent to the NURBS surface (10) if

$$\mathcal{N}_i = \sum_{j=1}^{\tau} m_{i,j} \mathcal{T}_j. \tag{13}$$

This relationship can be written in matrix form:

$$M\mathbb{T} = \mathbb{P} \tag{14}$$

where $\mathbb{T} = [\mathcal{T}_1, \mathcal{T}_2, \cdots, \mathcal{T}_\tau]^T$ is a column vector of T-spline homogeneous control points $\mathcal{T}_i$ and $\mathbb{P} = [\mathcal{N}_1, \mathcal{N}_2, \cdots, \mathcal{N}_\nu]^T$ is a column vector of NURBS homogeneous control points $\mathcal{N}_i$, and M is a $\nu \times \tau$ matrix with elements $m_{j,i}$. We call M the *T-spline-to-NURBS transform matrix*.

M also expresses how the T-spline basis functions are linear combinations of NURBS basis functions. From (11),

$$(T_1(s,t), T_2(s,t), \cdots, T_\tau(s,t)) = (N_1(s,t), N_2(s,t), \cdots, N_\nu(s,t))\, M \tag{15}$$

3.1. Computing the elements of M

The $m_{j,i}$ elements of M are found by performing knot insertion into the $T_i(s,t) = B[\vec{\mathbf{s}}_i](s) B[\vec{\mathbf{t}}_i](t)$ basis functions. This is accomplished by inserting into $B[\vec{\mathbf{s}}_i](s)$ all knots that are in $\vec{\mathbf{s}}$ but not in $\vec{\mathbf{s}}_i$, and inserting into $B[\vec{\mathbf{t}}_i](t)$ all knots that are in $\vec{\mathbf{t}}$ but not in $\vec{\mathbf{t}}_i$. This yields

$$B[\vec{\mathbf{s}}_i](s) = \sum_{j=1}^{c} d_i^j B_j(s) \quad \text{and} \quad B[\vec{\mathbf{t}}_i](t) = \sum_{k=1}^{r} e_i^k B_k(t) \tag{16}$$

where the values of d_i^j and e_i^k result from knot insertion. We will illustrate this process using

$$T_{31}(s,t) = B[s_1, s_4, s_6, s_8, s_{10}](s) \cdot B[t_1, t_3, t_6, t_9, t_{10}](t)$$

from the example in Figure 2.a. Into $B[\vec{\mathbf{s}}_{31}](s) = B[s_1, s_4, s_6, s_8, s_{10}](s)$ we

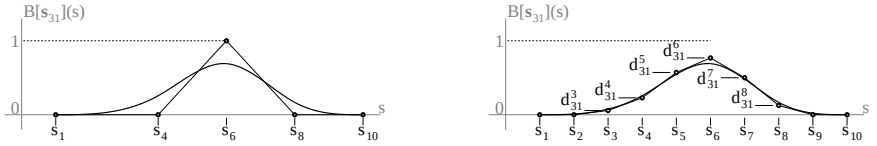

(a) Before refinement.

(b) After inserting knots at s_2, s_3, s_5, s_7, and s_9.

Figure 3: Basis function $B[\vec{\mathbf{s}}_{31}](s)$ before and after refinement.

insert s_2, s_3, s_5, s_7, and s_9 and into $B[\vec{\mathbf{t}}_{31}](t) = B[t_1, t_3, t_6, t_9, t_{10}](t)$ we insert t_2, t_4, t_5, t_7, and t_8. The result of insertion into $B[\vec{\mathbf{s}}_{31}](s)$ is illustrated in Figure 3 where the basis functions are drawn as explicit B-Spline curves.

Substituting (16) into (3),

$$T_i(s,t) = \sum_{j=1}^{c} \sum_{k=1}^{r} d_i^j e_i^k B_j(s) B_k(t). \tag{17}$$

Substituting (8) into (17) gives

$$T_i(s,t) = \sum_{j=1}^{c} \sum_{k=1}^{r} d_i^j e_i^k N_{jk}(s,t). \tag{18}$$

Comparing (18) with (11), we obtain the elements of M:

$$m_{\eta(j,k),i} = d_i^j e_i^k. \tag{19}$$

4. Determination of linear independence

We will refer to the expressions $w_i T_i(s,t) / \sum_{i=1}^{\tau} w_i T_i(s,t)$ in (1) as *rational* basis functions. When we ask whether a given T-spline is linearly independent, we are asking if the rational basis functions are linearly independent.

Rational basis functions are determined by the T-mesh topology, knot intervals, and weights. For a given topology, knot intervals, and weights, the set of all rational basis functions form a linear space. If the rational basis functions are linearly independent, they form a basis of the space, whose dimension is τ. Notice that for strictly positive weights w_i (which is assumed in practice), linear independence of the basis functions is equivalent to linear independence of the rational basis functions. This means that the choice of (strictly positive) weights does not affect linear independence.

4.1. A necessary and sufficient condition for linear independence

M contains information about linear independence, as expressed in the following theorem.

Theorem 1. *The T-spline-to-NURBS transform matrix M for any T-spline surface is unique. Furthermore, a necessary and sufficient condition for a T-spline to be linearly independent is that M is full rank.*

Proof. Referring to (15), since the $N_j(s,t)$ are B-spline *basis* functions, each column of M is unique, and so M itself is also unique.

By definition, T-spline basis functions are linearly independent if and only if there do not exist constants δ_i, not all zero, such that

$$\delta_1 T_1(s,t) + \cdots + \delta_\tau T_\tau(s,t) = (\delta_1, \cdots, \delta_\tau) \begin{pmatrix} T_1(s,t) \\ \vdots \\ T_\tau(s,t) \end{pmatrix} = 0.$$

From (15), this means that linear dependence requires

$$(\delta_1, \cdots, \delta_\tau) \begin{pmatrix} T_1(s,t) \\ \vdots \\ T_\tau(s,t) \end{pmatrix} = (\delta_1, \cdots, \delta_\tau) M^T \begin{pmatrix} N_1(s,t) \\ \vdots \\ N_\nu(s,t) \end{pmatrix} = 0.$$

Since $\{N_i(s,t)\}$ is a basis, the necessary and sufficient condition for linear dependence of the T-spline basis functions becomes

$$(\delta_1, \cdots, \delta_\tau)\, M^T = M \begin{pmatrix} \delta_1 \\ \vdots \\ \delta_\tau \end{pmatrix} = 0$$

for δ_i not all zero. But this will only happen if M is not full rank. □

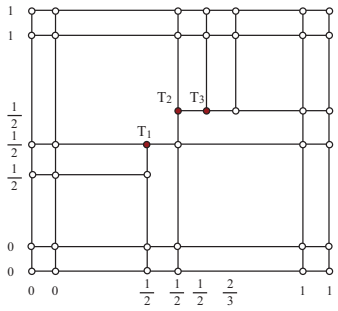

Figure 4: A linearly dependent T-spline.

Examples. In our experience, linearly dependent T-splines are very rare. However, Figure 4 shows an example of a linearly dependent T-spline, taken from (Buffa et al., 2010), where the numbers on the left and on the bottom are the knots. The matrix M in this case has a size of 56×40 and its rank is 39, so this T-spline is linearly dependent. As shown in (Buffa et al., 2010), the basis functions T_1, T_2 and T_3 satisfy a linear relationship: $T_1(s,t) = T_2(s,t) + \frac{1}{3}T_3(s,t)$.

4.2. Column reduction

Recall that the dimension of the null space of a matrix is called its *nullity* and that for a $\nu \times \tau$ matrix M, $\nu \geq \tau$, the Rank-nullity theorem states that the nullity of M is $\tau - \text{rank}(M)$. Thus, T-spline linear independence is equivalent the nullity of M being zero.

In cases where knot values are specified, nullity can be computed using standard numerical methods such as QR decomposition. However, we gain more insight if we leave the knots as variables. This will allow us, later in this section, to see how some T-spline mesh topologies can be linearly dependent for certain choices of knot intervals, but not for general choices of knots. This will also lead, in Section 5, to a directed graph representation that illuminates the relationship between nullity and the topology of a T-mesh, and in Section 6 to a proof that analysis-suitable T-splines are linearly independent for any choice of knots. Our approach is based on systematically eliminating rows and columns of M, producing a sequence of matrices whose nullity equals that of M.

If column i of M has a non-zero element m_{ji} and all other elements of row j are zero, we will call column i an *innocuous* column. *Column reduction*

is the operation of removing an innocuous column from M along with any zero rows that the column removal may have introduced. An *iteration of column reductions* is the process of identifying all innocuous columns of M and performing column reduction on all of those columns. Letting $M^0 = M$, a column reduction iteration on matrix M^i yields a smaller matrix M^{i+1}. We continue iterating until we create M^h which does not have innocuous columns.

Lemma 2. *Nullity of a $\nu \times \tau$ matrix with $\nu \geq \tau$ is invariant under column reduction.*

Proof. Follows from the Rank-nullity theorem. □

Corollary 3. *A series of column reduction iterations produces a sequence of matrices M^0, M^1, $\ldots M^h$, each of which has the same nullity.*

In the case where $M^h = \emptyset$, the nullity of M is zero. Thus we have

Corollary 4. *If a series of column reduction iterations yields $M^h = \emptyset$, the T-spline is linearly independent regardless of the choice of knots.*

The T-spline in Figure 2.a provides a good example of how column reduction can simplify the determination of nullity. After several iterations of column reduction, M^k vanishes, so the surface is linearly independent for all valid choices of knots.

While column reduction may not terminate in an empty matrix, it usually reduces the size of the matrix significantly, which facilitates the analysis of nullity. In particular, it can help in identifying knots that make the nullity of M zero or not.

For example, let us revisit the example from (Buffa et al., 2010) of a linearly dependent T-spline, treating the knots as variables. Assume the s knot vector is $[s_0, s_1, s_2, s_3, s_4, s_5, s_6, s_7]$ and the t knot vector is $[t_0, t_1, t_2, t_3, t_4, t_5, t_6]$ where $(s_0, t_0) = (0, 0)$ is the lower-left corner of the pre-image. The matrix M is initially size 56×40. After column reduction, we obtain a 6×3 matrix:

$$M^h = \begin{bmatrix} \frac{t_4 - t_1}{t_5 - t_1} & \frac{(t_2 - t_1)s_2}{(t_5 - t_1)s_4} & 0 \\ \frac{(t_4 - t_1)(s_6 - s_4)}{(t_5 - t_1)(s_6 - s_1)} & \frac{(t_2 - t_1)(s_5 - s_2)}{(t_5 - t_1)(s_5 - s_1)} & \frac{(t_2 - t_1)(s_2 - s_1)}{(t_5 - t_1)(s_5 - s_1)} \\ \frac{(t_4 - t_1)(s_6 - s_4)(s_6 - s_5)}{(t_5 - t_1)(s_6 - s_1)(s_6 - s_2)} & 0 & \frac{t_2 - t_1}{t_5 - t_1} \\ \frac{t_6 - t_4}{t_6 - t_2} & \frac{s_2}{s_4} & 0 \\ \frac{(t_6 - t_4)(s_6 - s_4)}{(t_6 - t_2)(s_6 - s_1)} & \frac{s_5 - s_2}{s_5 - s_1} & \frac{s_2 - s_1}{s_5 - s_1} \\ \frac{(t_6 - t_4)(s_6 - s_4)(s_6 - s_5)}{(t_6 - t_2)(s_6 - s_1)(s_6 - s_2)} & 0 & 1 \end{bmatrix}$$

A necessary and sufficient condition for M^h to have non-zero nullity is for all of its 3×3 minors to vanish. The minor that takes the first, fourth and sixth rows is $\frac{(t_4-t_2)(t_6-t_1)}{(t_5-t_1)(t_6-t_2)}$. To make this minor vanish, t_4 must be equal t_2, which implies a triple knot. Similarly, we can find that s_2 must equal s_4. If either one does not hold, the nullity is zero. Thus the corresponding T-spline is linearly dependent if and only if $s_2 = s_3 = s_4$ and $t_2 = t_3 = t_4$.

5. Directed graph representation

The discussion in Section 4 is algebraic in nature. We now describe a way to visualize the relationship between the T-mesh topology, the matrix M, and the column reduction operation using a directed graph G. This will enable us to identify topological conditions for a T-mesh that assure linear independence, regardless of knot values.

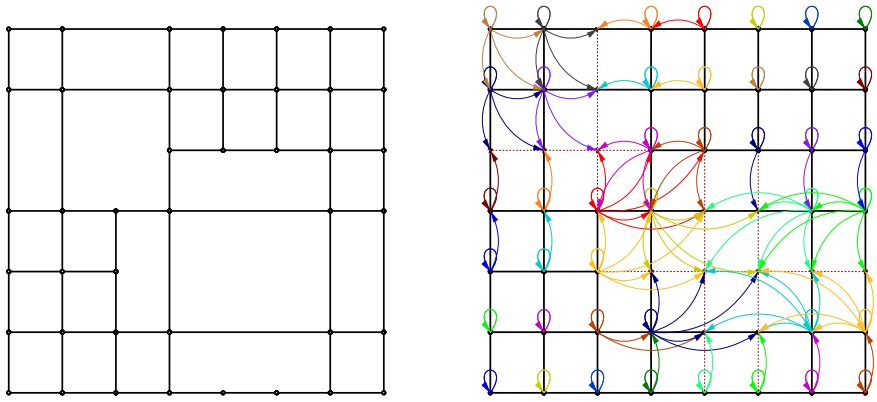

(a) T-mesh. (b) Corresponding directed graph G.

Figure 5: A T-mesh and its directed graph.

Figure 5.b shows the directed graph G for the T-mesh in Figure 5.a. G contains two types of nodes: *T-nodes* correspond to T-spline control points, and *N-nodes* correspond to control points of the underlying NURBS. A T-node and an N-node that have the same central knot indices are said to correspond to each other. The N-nodes lie in a rectangular grid, and each T-node is drawn on top of its corresponding N-node. This would make it confusing to distinguish between T-nodes and N-nodes, were it not for the

fact that the edges in the directed graph G always originate at T-nodes and terminate at N-nodes. Edges represent the non-zero elements of M: If element m_{ij} is non-zero, an edge is drawn from T-node j to N-node i. Thus, each T-node always points to its corresponding N-node, creating edges that are small loops.

The *footprint* of a T-node is the set of N-nodes that the T-node points to. The footprint of $\mathbf{T}_i$ consists of all $\mathbf{N}_{jk}$ for which $d_i^j e_i^k \neq 0$ (see (19)). Those (j,k) pairs can be determined by examining the knot vectors associated with the T-node's basis function. Denote those knot vectors

$$[s_{\sigma_j^0}, s_{\sigma_j^1}, s_{\sigma_j^2}, s_{\sigma_j^3}, s_{\sigma_j^4}] \quad \text{and} \quad [t_{\tau_k^0}, t_{\tau_k^1}, t_{\tau_k^2}, t_{\tau_k^3}, t_{\tau_k^4}]. \tag{20}$$

If there are no multiple knots in (20), $d_i^j \neq 0$ for $\sigma_i^0 + 1 < j < \sigma_i^4 - 1$. This property is illustrated in Figure 3. Similarly, $e_i^k \neq 0$ for $\tau_i^0 + 1 < k < \tau_i^4 - 1$. So, if there are no multiple knots in knot vectors (20), the footprint of $\mathbf{T}_i$ consists of the rectangular grid of N-nodes

$$\{\mathbf{N}_{jk} \mid \ \sigma_i^0 + 1 < j < \sigma_i^4 - 1 \quad \text{and} \quad \tau_i^0 + 1 < k < \tau_i^4 - 1\}.$$

The footprints of the T-nodes in Figure 5.a are evident from the sets of edges emanating from each T-node in the directed graph in Figure 5.b.

The *valence* of an N-node is the number of edges that point to it. The valence of a T-node is the number of edges originating from it. An *innocuous node* is any T-node that points to at least one N-node of valence one; this is the graphical equivalent of an innocuous column of M. A *subgraph* of G consists of any set of T-nodes along with all N-nodes pointed to by those T-nodes, and all edges connecting those nodes.

The operation of *pruning* a graph consists of eliminating all innocuous nodes in the graph. The pruned graph then consists of the remaining T-nodes, the edges originating from those T-nodes, and the N-nodes pointed to. Pruning is the graphical equivalent of column reduction of M. Pruning usually creates new innocuous nodes, which invites a second pruning. Pruning continues until no innocuous nodes remain. We call the resulting graph a fully pruned graph. Figure 6 shows the result of the first, second, and third prunings for the graph in Figure 5. The graph in Figure 6.c is fully pruned.

A *V2-subgraph* is any subgraph whose N-nodes have a valence of at least two. A sequence of prunings either terminates in an empty graph, or in one or more V2-subgraphs. The prunings in Figure 6 terminate in a V2-subgraph that consists of three T-nodes and six N-nodes.

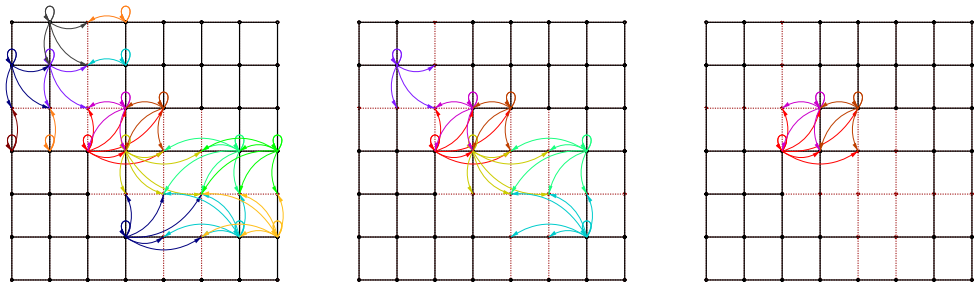

(a) After first pruning. (b) After second pruning. (c) After third pruning.

Figure 6: First, second and third (final) prunings.

Theorem 5. *Any T-spline whose T-mesh contains no V2-subgraphs is linearly independent for all choices of knots.*

Proof. Since pruning is the graphical visualization of column reduction of M, Corollary 4 proves this theorem. □

Pruning provides an algorithm for discovering all V2-subgraphs in a graph: a fully pruned graph is either empty, or consists of one or more disjoint V2-subgraphs. However, V2-subgraphs can also be identified directly using

Lemma 6. *The footprints of all T-nodes in a V2-subgraph $\tilde{G}$ cover each N-node in $\tilde{G}$ at least twice.*

6. Linear independence of analysis-suitable T-splines

This section studies an important subset of T-splines called analysis-suitable T-splines. The ultimate result is Theorem 18: Analysis-suitable T-splines are linearly independent. Most of this section sets the stage for proving this theorem, which involves showing that T-meshes for analysis-suitable T-splines have no V2-subgraphs.

Definition 7. *An analysis-suitable T-mesh is one for which no horizontal T-junction extension intersects a vertical T-junction extension. An analysis-suitable T-spline is one whose T-mesh is analysis-suitable.*

A T-junction is a T-node that has three edges connected to it, with one missing edge. A T-junction extension is a closed line segment that extends

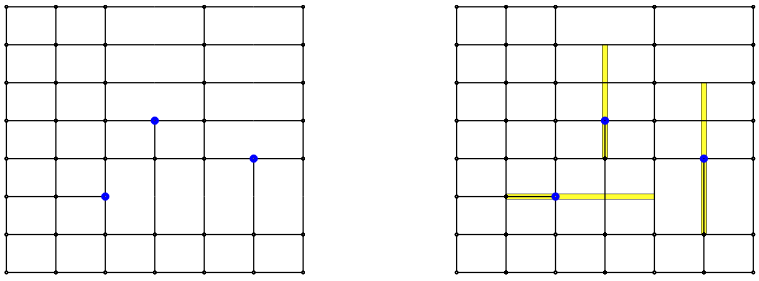

(a) T-mesh with three T-junctions.

(b) Extentions shown in yellow.

Figure 7: T-junction extensions.

across two rectangles in the direction of the missing edge, and in the other direction to the first-encountered T-node or orthogonal edge. T-junction extensions are illustrated in Figure 7. Since extensions are closed line segments, a horizontal and vertical extension can intersect either on the interior of both extensions (as in Figure 8.a) or at the endpoint of one or both extensions (as in Figure 8.b).

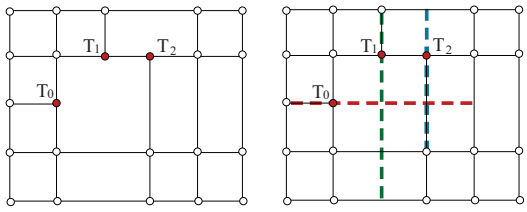

(a) Extensions that cross.

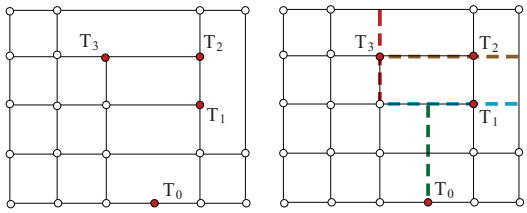

(b) Extensions that touch.

Figure 8: Extensions that violate the analysis-suitable T-mesh conditions.

Generic T-splines allow several special node configurations other than T-junctions. For example, point $\mathbf{T}_1$ in Figure 9.a is a conventional valence four

control point, $\mathbf{T}_2$ is a valence three T-junction, $\mathbf{T}_3$ is called a valence two T-junction, $\mathbf{T}_4$ is an L-junction, $\mathbf{T}_5$ is an I-junction, and $\mathbf{T}_6$ is an isolated node. Figure 9.b shows the extensions for these various types of T-nodes.

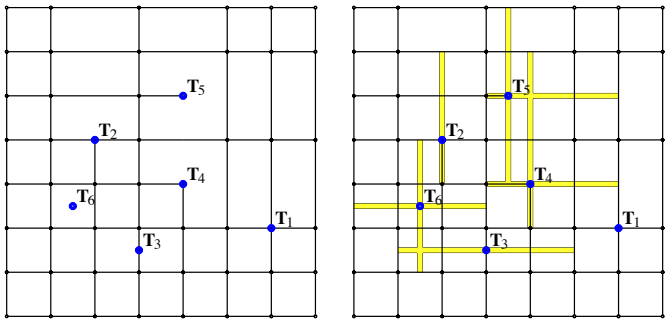

(a) Several types of T-nodes.

(b) Extensions.

Figure 9: T-nodes and Extensions.

Lemma 8. *A T-mesh that has an L-junction, I-junction, or isolated node has T-junction extensions that cross.*

Proof. As is evident from Figure 9, L-junctions, I-junctions, and isolated nodes each have both a horizontal and vertical extension that intersect each other. □

Corollary 9. *Analysis-suitable T-splines can have no L-junctions, I-junctions, or isolated nodes.*

Proof. Follows directly from Definition 7 and Lemma 8 □

However, valence two T-junctions such as $\mathbf{T}_3$ in Figure 9 are permitted in an analysis-suitable T-spline.

Definition 10. *A* symbol array *describes the topology of a T-mesh by assigning one of the ten following symbols to each node of the T-mesh's directed graph. If an N-node has a corresponding T-node, just one symbol is assigned to the pair of them. The symbols describe topological elements in the T-mesh (other than L-junctions, I-junctions, and isolated nodes), as illustrated in*

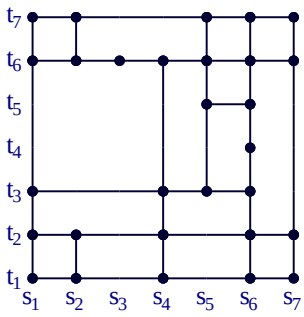

(a) T-mesh.

t_7	+	+	−	−	+	+	+
t_6	+	⊥	=	⊤	+	+	+
t_5	|	.	.	|	⊢	⊣	|
t_4	|	.	.	|	|	‖	|
t_3	+	−	−	+	⊥	⊣	|
t_2	+	+	−	+	−	+	+
t_1	+	+	−	+	−	+	+
	s_1	s_2	s_3	s_4	s_5	s_6	s_7

(b) Symbol array.

Figure 10: A T-mesh and its corresponding symbol array.

Figure 10.

+	*Valence four T-node, or boundary T-node*
$\vdash$, $\dashv$, $\perp$, $\top$	*Valence three T-junction*
$\|\|$	*Vertical valence-two T-junction*
$=$	*Horizontal valence-two T-junction*
$\|$	*Vertical edge node*
$-$	*Horizontal edge node*
$\cdot$	*Does not correspond to a T-node or edge in the T-mesh*

To each N-node N_{ij} we assign a symbol $\mathbb{S}_{ij}$. For example, in Figure 10, $\mathbb{S}_{2,6} = \perp$ and $\mathbb{S}_{6,4} = \|$.

Nodes with symbols "|" or "−" correspond to edges in the T-mesh and are called edge nodes. Nodes with symbols $+, \vdash, \dashv, \perp, \top, \|, =$ connote various types of T-nodes in the T-mesh and are called, collectively, T-nodes.

Lemma 11. *Legal neighbors for T-meshes that have no L-junctions, I-junctions,*

or isolated nodes are listed in this table.

$\mathbb{S}_{i,j}$	$\mathbb{S}_{i+1,j} \in$	$\mathbb{S}_{i,j+1} \in$	$\mathbb{S}_{i-1,j} \in$	$\mathbb{S}_{i,j-1} \in$
$+$	$\{+,\dashv,\perp,\top,=,-\}$	$\{+,\vdash,\dashv,\top,\|\|,\|\}$	$\{+,\vdash,\perp,\top,=,-\}$	$\{+,\vdash,\dashv,\perp,\|\|,\|\}$
$\vdash$	$\{+,\dashv,\perp,\top,=,-\}$	$\{+,\vdash,\dashv,\top,\|\|,\|\}$	$\{\|,\cdot\}$	$\{+,\vdash,\dashv,\perp,\|\|,\|\}$
$\dashv$	$\{\|,\cdot\}$	$\{+,\vdash,\dashv,\top,\|\|,\|\}$	$\{+,\vdash,\perp,\top,=,-\}$	$\{+,\vdash,\dashv,\perp,\|\|,\|\}$
$\perp$	$\{+,\dashv,\perp,\top,=,-\}$	$\{+,\vdash,\dashv,\top,\|\|,\|\}$	$\{+,\vdash,\perp,\top,=,-\}$	$\{-,\cdot\}$
$\top$	$\{+,\dashv,\perp,\top,=,-\}$	$\{-,\cdot\}$	$\{+,\vdash,\perp,\top,=,-\}$	$\{+,\vdash,\dashv,\perp,\|\|,\|\}$
$\|\|$	$\{\|,\cdot\}$	$\{+,\vdash,\dashv,\top,\|\|,\|\}$	$\{\|,\cdot\}$	$\{+,\vdash,\dashv,\perp,\|\|,\|\}$
$=$	$\{+,\dashv,\perp,\top,=,-\}$	$\{-,\cdot\}$	$\{+,\vdash,\perp,\top,=,-\}$	$\{-,\cdot\}$
$\|$	$\{\vdash,\|\|,\|,\cdot\}$	$\{+,\vdash,\dashv,\top,\|\|,\|\}$	$\{\dashv,\|\|,\|,\cdot\}$	$\{+,\vdash,\dashv,\perp,\|\|,\|\}$
$-$	$\{+,\dashv,\perp,\top,=,-\}$	$\{\perp,=,-,\cdot\}$	$\{+,\vdash,\perp,\top,=,-\}$	$\{\top,=,-,\cdot\}$
$\cdot$	$\{\vdash,\|\|,\|,\cdot\}$	$\{\perp,=,-,\cdot\}$	$\{\dashv,\|\|,\|,\cdot\}$	$\{\top,=,-,\cdot\}$

Proof. These relationships can be verified by considering each pair of neighboring symbols and observing which pairs are topologically possible. □

The notation $[\mathbb{S}_{i,j}, \mathbb{S}_{k,j})$, $i < k$ will be used in two related ways: It can denote the horizontal sequence of symbols, $\mathbb{S}_{i,j}, \ldots, \mathbb{S}_{k-1,j}$, or the set of symbols $\{\mathbb{S}_{i,j}, \ldots, \mathbb{S}_{k-1,j}\}$. Likewise, the notation $(\mathbb{S}_{i,j}, \mathbb{S}_{i,k})$, $j < k$, can mean either the vertical sequence of symbols $\mathbb{S}_{i,j+1}, \ldots, \mathbb{S}_{i,k-1}$, or the set of symbols $\{\mathbb{S}_{i,j+1}, \ldots, \mathbb{S}_{i,k-1}\}$. The meanings will be clear from the context. In Figure 10.b, for example, $[N_{1,2}, N_{7,2}]$ can mean either $+, +, -, +, -, +, +$, or $\{+, -\}$; and $(N_{5,2}, N_{5,6}]$ can mean either $\perp, |, \vdash, +$ or $\{\perp, |, \vdash, +\}$.

A *K-node* with respect to a T-node $\mathbf{T}$ is an N-node that determines an s or t knot value for $\mathbf{T}$'s basis function. In Figure 11.a, the labelled N-nodes are K-nodes with respect to $\mathbf{T}$. The K-nodes for determining s knot values (called s-K-nodes) are either T-nodes or vertical edge nodes. The K-nodes for determining t knot values (called t-K-nodes) are either T-nodes or horizontal edge nodes.

The K-nodes define a 4×4 grid of rectangles, as illustrated by the rectangles bounded by red lines in Figure 11.b. The union of the four rectangular regions adjacent to $\mathbf{T}$ (shaded yellow) is called the *one-neighborhood* of the domain of $\mathbf{T}$, and the union of the other 12 rectangles (shaded green) is called the *two-neighborhood* of the domain of $\mathbf{T}$. The bounding edges are considered part of the neighborhood. Thus, the boundary between the one- and two-neighborhoods lies in both neighborhoods.

Corollary 12. *Lemma 11 leads to the following topological constraints for a T-mesh that has no L-junctions, I-junctions, or isolated nodes.*

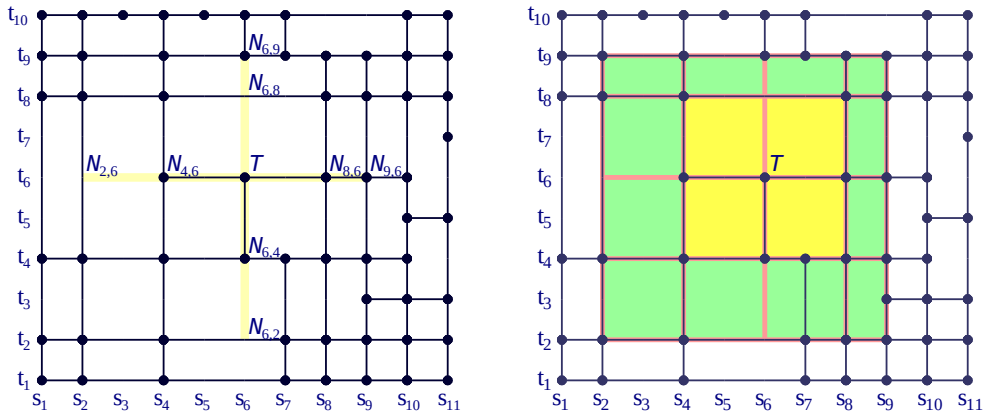

(a) K-nodes for $\mathbf{T}$. (b) One- and two-neighborhoods for $\mathbf{T}$.

Figure 11: K-nodes and neighborhoods.

a. *If* $\mathbb{S}_{a,b} \in \{\cdot, -, \top, =\}$ *and* $\mathbb{S}_{a,c}$ *is a T-node,* $a < b < c$*, and there are no T-nodes in* $(\mathbb{S}_{a,b}, \mathbb{S}_{a,c})$*, then* $\mathbb{S}_{a,c} \in \{=, \perp\}$.

b. *If* $\mathbb{S}_{a,c} \in \{\cdot, |, \dashv, \|\}$ *and* $\mathbb{S}_{b,c}$ *is a T-node,* $b > a$*, and there are no T-nodes in* $(\mathbb{S}_{a,c}, \mathbb{S}_{b,c})$*, then* $\mathbb{S}_{b,c} \in \{\vdash, \|\}$.

c. *If* $\mathbb{S}_{a,c}$ *and* $\mathbb{S}_{b,c}$ *are adjacent s-K-nodes with respect to a T-node* $\mathbb{S}_{d,c}$*, where* $b > a$ *and* $d \notin (a, b)$*, then* $(\mathbb{S}_{a,c}, \mathbb{S}_{b,c}) \subset \{\cdot, -\}$.

d. *If* $\mathbb{S}_{a,b}$ *and* $\mathbb{S}_{a,c}$ *are adjacent t-K-nodes with respect to a T-node* $\mathbb{S}_{a,d}$*,* $c > b$ *and* $d \notin (b, c)$*, then* $(\mathbb{S}_{a,b}, \mathbb{S}_{a,c}) \subset \{\cdot, |\}$.

e. *If* $\mathbb{S}_{a,b} \in \{\cdot, -\}$ *and* $\mathbb{S}_{a,c}$ *is an s-K-node,* $c > b$*, and there are no T-nodes in* $(\mathbb{S}_{a,b}, \mathbb{S}_{a,c})$*, then* $\mathbb{S}_{a,c} \in \{=, \perp\}$.

f. *If* $\mathbb{S}_{a,c} \in \{\cdot, |\}$ *and* $\mathbb{S}_{b,c}$ *is a t-K-node,* $b > a$*, and there are no T-nodes in* $(\mathbb{S}_{a,c}, \mathbb{S}_{b,c})$*, then* $\mathbb{S}_{b,c} \in \{\|, \vdash\}$.

g. *If* $\mathbb{S}_{a,b} \in \{\cdot, -\}$ *and* $\mathbb{S}_{a,c}$ *is an s-K-node,* $c > b$*, there is at least one T-node in* $(\mathbb{S}_{a,b}, \mathbb{S}_{a,c}]$*. For the T-node with the smallest value of* d*,* $b < d \leq c$*,* $\mathbb{S}_{a,d} \in \{=, \perp\}$.

h. *If* $\mathbb{S}_{a,c} \in \{\cdot, |\}$ *and* $\mathbb{S}_{b,c}$ *is a t-K-node,* $b > a$*, there is at least one T-node in* $(\mathbb{S}_{a,c}, \mathbb{S}_{b,c}]$*. For the T-node with the smallest value of* d*,* $a < d \leq b$*,* $\mathbb{S}_{d,c} \in \{\|, \vdash\}$.

i. *If a T-node with central knots indices (b, e) has a one-neighborhood bounded by knot lines s_a, s_c, t_d, t_f with $a < b < c$ and $d < e < f$, then*
$(\mathbb{S}_{a,d}, \mathbb{S}_{b,d}) \bigcup (\mathbb{S}_{b,d}, \mathbb{S}_{c,d}) \subset \{\cdot, -, =, \top\}$;
$(\mathbb{S}_{a,f}, \mathbb{S}_{b,f}) \bigcup (\mathbb{S}_{b,f}, \mathbb{S}_{c,f}) \subset \{\cdot, -, =, \bot\}$;
$(\mathbb{S}_{a,d}, \mathbb{S}_{a,e}) \bigcup (\mathbb{S}_{a,e}, \mathbb{S}_{a,f}) \subset \{\cdot, |, \|, \dashv\}$;
$(\mathbb{S}_{c,d}, \mathbb{S}_{c,e}) \bigcup (\mathbb{S}_{c,e}, \mathbb{S}_{c,f}) \subset \{\cdot, |, \|, \vdash\}$.

j. *If there are no T-nodes in $(\mathbb{S}_{a,b}, \mathbb{S}_{a,c})$ and $\mathbb{S}_{a,c} \in \{\cdot, -\}$, $c > b$, then $\mathbb{S}_{a,b} \in \{\cdot, -, =, \top\}$.*

k. *If $\mathbb{S}_{a,b}$ is an s-K-node, and $\mathbb{S}_{a,c} \in \{\cdot, -, =, \top\}$, $c > b$, there is at least one T-node in $[\mathbb{S}_{a,b}, \mathbb{S}_{a,c}]$. For the T-node with the largest value of d, $b \leq d \leq c$, $\mathbb{S}_{a,d} \in \{=, \top\}$.*

Proof. These can be confirmed by repeated application of Lemma 11. □

Lemma 13. *Given a rectangular region R, bounded by knot lines s_a, s_c, t_b, t_d ($a < c$ and $b < d$), in a symbol array for a T-mesh that satisfies one of these two conditions:*

- *Either $(\mathbb{S}_{a,b}, \mathbb{S}_{c,b}) \subset \{\cdot, -\}$ or $(\mathbb{S}_{a,d}, \mathbb{S}_{c,d}) \subset \{\cdot, -\}$, and either $(\mathbb{S}_{c,b}, \mathbb{S}_{c,d}) \subset \{\cdot, |, \|, \dashv\}$ or $(\mathbb{S}_{a,b}, \mathbb{S}_{a,d}) \subset \{\cdot, |, \|, \vdash\}$,*
- *Either $(\mathbb{S}_{c,b}, \mathbb{S}_{c,d}) \subset \{\cdot, |\}$ or $(\mathbb{S}_{a,b}, \mathbb{S}_{a,d}) \subset \{\cdot, |\}$, and either $(\mathbb{S}_{a,d}, \mathbb{S}_{c,d}) \subset \{-, \cdot, =, \top\}$ or $(\mathbb{S}_{a,b}, \mathbb{S}_{c,b}) \subset \{-, \cdot, =, \bot\}$,*

if there exists a T-node in the interior of R, the T-mesh has intersecting extensions.

Proof. If the T-mesh has L-junctions, I-junctions or isolated T-nodes, Lemma 8 assures the existence of intersecting extensions, so our proof assumes that there are no L-junctions, I-junctions or isolated T-nodes. Our proof uses the conditions $(\mathbb{S}_{a,d}, \mathbb{S}_{c,d}) \subset \{\cdot, -\}$ and $(\mathbb{S}_{c,b}, \mathbb{S}_{c,d}) \subset \{\cdot, |, \|, \dashv\}$. Proofs involving the other conditions are similar.

Assume the existence of one or more T-nodes in the interior of R. Choose the highest T-node (if there are more than one T-node on that t-knot line, choose the rightmost of them) and denote it by **T**, with central knot indices (i, j). Reasoning from Lemma 11, $\mathbb{S}_{i,j+1} \neq |$ because $\mathbb{S}_{i,d} \in \{\cdot, -\}$ and there are no T-nodes in $(\mathbb{S}_{i,j}, \mathbb{S}_{i,d})$. Thus, $\mathbb{S}_{i,j} \in \{=, \top\}$. Since **T** was chosen to assure that no T-nodes are in $(\mathbb{S}_{i,j}, \mathbb{S}_{c,j})$ and again reasoning from Lemma 11, $(\mathbb{S}_{i,j}, \mathbb{S}_{c,j}) = \{-\}$ and $\mathbb{S}_{c,j} = \dashv$. $N_{c,j}$ and **T** have intersecting T-junction extensions. □

Lemma 14. *If a T-mesh has no L-junctions, I-junctions, or isolated nodes, there is no T-node in the interior of the one-neighborhood of the domain of a T-node* $\mathbf{T}$*, other than* $\mathbf{T}$ *itself.*

Proof. Suppose there exists a T-node $\mathbf{P}$ in the interior of the one-neighborhood of the domain of a T-node T. $\mathbf{P}$ cannot be on one of the four edges incident to T because a T-node on the edges incident to T is a K-node. Thus $\mathbf{P}$ must be in the interior of the four rectangles adjacent to T. Without loss of generality, we assume that $\mathbf{P}$ lies in the interior of the north-east rectangle adjacent to T. Furthermore, we can assume $\mathbf{P}$ is the lowest and then left-most T-node in this rectangle. Thus there is no edge connecting to $\mathbf{P}$ from below or from the left. Otherwise, the edge will hit the horizontal edge or the vertical edge incident to T and this will contradict the assumption that the rectangle is in the one-neighborhood of the domain of T. Thus $\mathbf{P}$ must be an L-junction, I-junction or isolated node, which violates the hypothesis. □

Lemma 15. *Given a T-mesh with T-nodes* $\mathbf{T}_1$ *and* $\mathbf{T}_2$ *with central knot indices* (i_1, j_1) *and* (i_2, j_2)*, where* $i_1 < i_2$ *and* $j_1 > j_2$*, if both T-nodes have the same vertical knot line for their leftmost K-nodes (i.e., the left vertical line in Figure 12) and the same horizontal knot line for their lowest K-nodes (i.e., the bottom horizontal line in Figure 12), then the T-mesh must have intersecting extensions.*

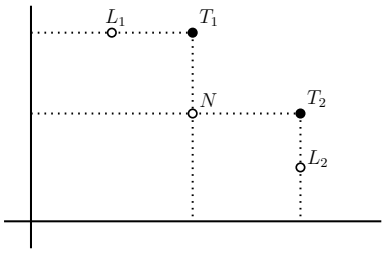

Figure 12: L_1 and L_2 are K-nodes for T-nodes T_1 and T_2, respectively. The left vertical line and the bottom horizontal line are the knot lines of the leftmost K-node and the lowest K-node of both T_1 and T_2.

Proof. If the T-mesh has any L-junctions, I-junctions, or isolated nodes, Lemma 8 shows that there must be intersection extensions, so our proof assumes there are no L-junctions, I-junctions, or isolated nodes.

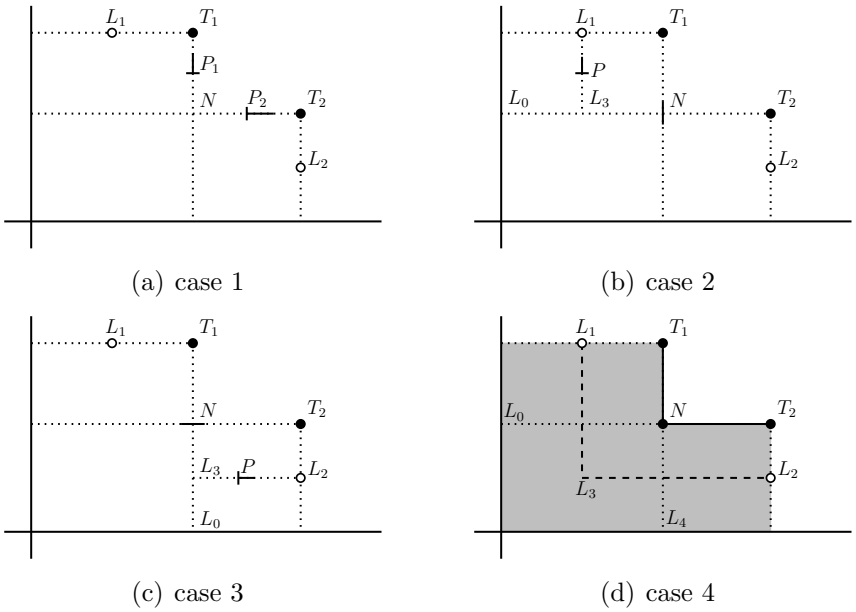

(a) case 1 (b) case 2

(c) case 3 (d) case 4

Figure 13: Four different cases of Figure 12.

With reference to Figure 12, we examine the intersection point N between the vertical line going through T_1 and the horizontal line going through T_2. We show that extensions intersect in each of four possible cases.

- **Case 1.** N is type "$\cdot$" (see Figure 13(a)). Denote by P_1 the lowest T-node between N and T_1 (there is at least one such T-node, since T_1 is a T-node). From Corollary 12.a, P_1 must be of type "$\perp$" or "$=$". Similarly, $(N, T_2]$ contains at least one T-node. Denote the leftmost such T-node by P_2. From Corollary 12.b, P_2 is of type "$\vdash$" or "$\|$". The T-junction extensions of P_1 and P_2 cross at N.

- **Case 2.** N is type "$|$" (see Figure 13(b)). In this case, L_0 and N are the two left K-nodes of T_2, so node L_3 cannot be a T-node or of type "$-$" and therefore $L_3 \in \{\cdot, -\}$. There is no T-node between N and T_2 so from Corollary 12.b, T_2 must be a T-junction of type "$\vdash$" or "$\|$". Since L_1 is a K-node of T_1, it must be a T-node or a node of type "$|$". $(L_3, L_1]$ contains at least one T-node. Denote the lowest one by P. From Corollary 12.a, $P \in \{\perp, =\}$. The T-junction extensions of P and T_2 intersect at L_3.

- **Case 3.** N is type "$-$" (see Figure 13(c)). Since Case 3 and Case 2 are symmetric, we can show similarly that the T-junction extensions of P and T_1 cross.

- **Case 4.** N is a T-node (see Figure 13(d)).

  Since N and L_0 are K-nodes for T_2, there is no T-node or node of type "$|$" between L_0 and N, or between T_2 and N. Similarly, since N and L_4 are K-nodes for T_1, there is no T-node or node of type "$-$" between L_4 and N, or between N and T_1. Therefore, the shaded region in Figure 13(d) is in the one-neighborhood of the domain of N. According to Lemma 14, there is no T-node in the shaded region.

  From Corollary 12.c and Corollary 12.e, $L_1 \in \{=, \perp\}$. From Corollary 12.d and Corollary 12.f, $L_2 \in \{\|, \vdash\}$. Thus L_1 and L_2 are T-junctions whose extensions cross at L_3.

□

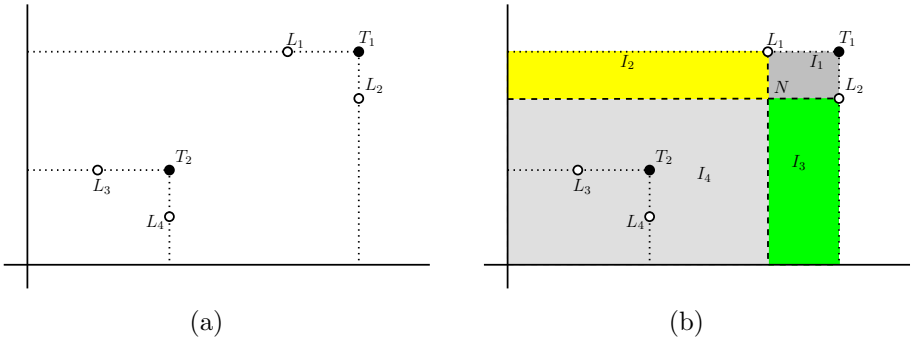

Figure 14: (a) L_1 and L_2 are K-nodes for T-node T_1. L_3 and L_4 are K-nodes for T-node T_2. The left vertical line and the bottom horizontal line are the knot lines of the leftmost K-node and the lowest K-node of both T_1 and T_2. (b). Four rectangles around the intersection node N.

Lemma 16. *Given a T-mesh with T-nodes* $\mathbf{T}_1$ *and* $\mathbf{T}_2$ *with central knot indices* (i_1, j_1) *and* (i_2, j_2)*, where* $i_1 > i_2$ *and* $j_1 > j_2$*, if both T-nodes have the same vertical knot line for their leftmost K-nodes (i.e., the left vertical line in Figure 14) and the same horizontal knot line for their lowest K-nodes (i.e., the bottom horizontal line in Figure 14), then the T-mesh must have intersecting extensions.*

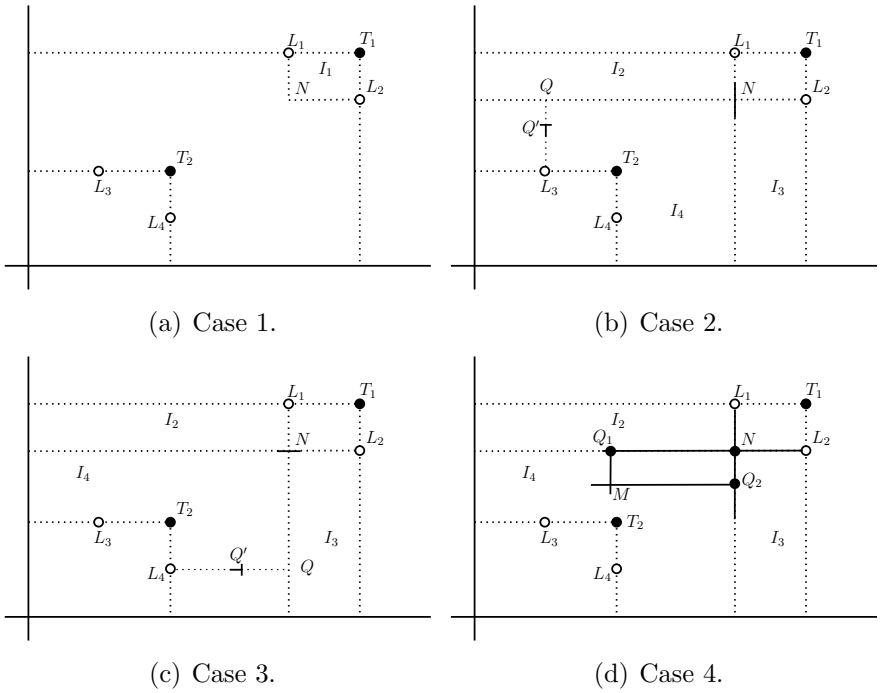

(a) Case 1. (b) Case 2.

(c) Case 3. (d) Case 4.

Figure 15: Four different cases of Figure 14.

Proof. If the T-mesh has any L-junctions, I-junctions or isolated nodes, the T-mesh has intersecting extensions. The remainder of the proof assumes there are no L-junctions, I-junctions or isolated nodes.

Referring to Figure 14(a), the vertical line going through K-node L_1 and the horizontal line going through K-node L_2 intersect at N-node N and divide the big rectangle into four smaller rectangles: I_1, I_2, I_3 and I_4 (see Figure 14(b)). I_1 is a one-neighborhood rectangle of T_1. According to Lemma 14, there is no T-node in the interior of I_1. Note that there is no T-node or node of type "|" in the interior of the top edge of I_2 and no T-node or node of type "−" in the interior of the right edge of I_3. According to Lemma 13, if I_2 or I_3 contain a T-node, there must be crossing extensions; so we assume they don't contain a T-node.

We now examine all six possible node types for N, and show that intersecting extensions are inevitable. Observe that since L_1 is a K-node, it is either a T-node, or of type "|", and since L_2 is a K-node, it is either a T-node, or of type "−".

- **Case 1.** N is type "$\cdot$". Referring to Figure 15(a), Corollaries 12.g and 12.i assure L_1 is type "$\perp$" or "$=$", and there are no other T-nodes in (N, L_1). From Corollaries 12.h and 12.i, L_2 is of type "$\vdash$" or "$\|$" and there are no other T-nodes in (N, L_2). The extensions of L_1 and L_2 cross at N.

- **Case 2.** N is a node of type "$|$" (see Figure 15(b)). From Corollaries 12.h and 12.i, L_2, is of type "$\vdash$" or "$\|$" and there are no other T-nodes in (N, L_2). We will now show that the extension of L_2 intersects the vertical extension of a T-junction in I_4. From Corollaries 12.j and 12.k, there exists a T-junction on $(L_3, Q]$ and the highest such T-junction (call it Q') is type "$\top$" or "$=$". The extension of Q' intersects the extension of L_2, unless there is a T-node in (Q, N). But from Corollary 12.j, any T-node in (Q, N) is of type "$\top$" or "$=$". The rightmost such T-node has an extension that intersects that of N.

- **Case 3.** N is a node of type "$-$" (see Figure 15(c)). Since Cases 2 and 3 are symmetric, the proofs are also symmetric.

- **Case 4.** N is type "$+$". The proof for Case 2 confirms that I_4 must contain a T-node. Therefore, Lemma 13 requires that there exist T-junctions Q_1 and Q_2 as illustrated in Figure 15(d), otherwise the T-node(s) in I_4 would cause crossing extensions. Corollary 12.j assures that Q_1 is of type "$\top$" or "$=$". Similarly, Q_2 must be of type "$\|$" or "$\dashv$". Choose Q_1 and Q_2 such that there are no T-nodes in (Q_1, N) and (Q_2, N). Corollary 12.i assures that either the extensions of Q_1 and Q_2 cross at M, or else if there is a T-node in (Q_1, M), it is a T-junction whose extension will cross with Q_1's extension, or else if there is a T-node in (Q_2, M), it is a T-junction whose extension will cross with Q_2.

- **Case 5.** N is a T-node of type "$\|$", "$\dashv$", or "$\vdash$". The major arguments for this proof are similar to those in Case 2, except we consider the extensions of N rather than the extensions of L_2.

- **Case 6.** N is a T-node of type "$=$", "$\top$", or "$\perp$". The major arguments for this proof are similar to those in Case 3, except we consider the extensions of N rather than the extensions of L_1.

□

Lemma 17. *N_{ij} is the lowest, then leftmost node in a V2-subgraph G. That is, for all other nodes $N_{kl} \in G$, $j \leq l$ and for all other nodes $N_{kj} \in G$, $i < k$. If a T-node $T \in G$ points to N_{ij}, where the central knot indices of T are (k, l), $k \geq i$ and $l \geq j$. That is, T is in the north-east region of N.*

Proof. The lemma can only be violated by a T-node $T \in G$ that points to N_{ij} where the central knot indices of T are (k, l), where $k < i$ and $l > j$. However, the lower-left corner of the footprint of T is N_{kj}, which is also in G. This contradicts the assumption. □

Now we are ready to present the main result of this section.

Theorem 18. *Analysis-suitable T-spline surfaces are linearly independent.*

Proof. We prove by contradiction that an analysis-suitable T-mesh does not contain a V2-subgraph. Assume the existence of a V2-subgraph G. Consider the lowest and then leftmost node in G, denoted by N. There are two possibilities:

- **Case 1.** N has no corresponding T-node. Then there exist at least two T-nodes in G pointing to N. Denote two such T-nodes by T_1 and T_2. By Lemma 17, T_1 and T_2 are in the north-east region of N.

  Furthermore, we can prove that both T_1 and T_2 must have the same leftmost and lowest knot lines of K-nodes. In fact, if we assume the knot line of the leftmost K-node of T_1 is on the left of that of T_2, there exists at least one vertical knot line between the knot line of the leftmost K-node of T_2 and N since N is covered by the footprint of T_2 (see Figure 16 for an illustration). Denote the s coordinate of this vertical knot line by s_0 and the knot coordinates of N by (s_1, t_1). Then $s_0 < s_1$ and the vertical knot line $s = s_0$ is on the right of the leftmost knot lines of K-nodes of T_1 and T_2. Therefore the node with coordinates (s_0, t_1) is covered by the footprint of T_1 and is thus in G, but it is on the left of N, which contradicts the assumption that N is the lowest and then leftmost node in G. Therefore T_1 and T_2 should have the same leftmost knot lines of K-nodes. In a similar way, we can prove that they have the same lowest knot lines of K-nodes.

  If T_1 and T_2 lie on the same vertical line, they cannot have the same lowest knot line of K-nodes. Similarly, T_1 and T_2 cannot lie on the same horizontal line. Therefore the relative relationship of these two

T-nodes must satisfy the conditions of either Lemma 15 or Lemma 16. However, both Lemmas have shown that there must exist intersecting extensions.

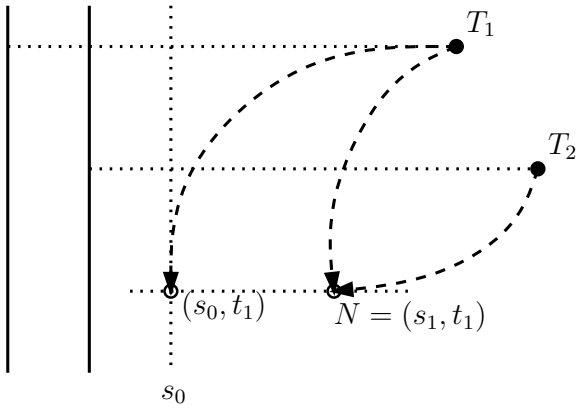

Figure 16: Two T-nodes have different knot lines of the leftmost K-nodes.

- **Case 2.** N is a T-node. There exists at least another T-node T in G which points to it. Similarly, by Lemma 17, T must be in the north-east region of N and we can also prove that both T and N have the same lowest and leftmost knot lines of K-nodes as we did for Case 1. Thus T and N cannot lie on the same vertical line or horizontal line, and by Lemma 16, there must exist intersecting extensions.

□

7. Conclusion

This paper presents algebraic and topological methods for analyzing linear independence of T-splines. We show that any T-spline whose T-mesh contains no V2-subgraphs is linearly independent for all choices of knots, and that analysis-suitable T-splines are always linearly independent because they contain no V2-subgraphs. Analysis-suitable T-splines thus provide a solid mathematical foundation for isogeometric analysis. Future papers will show that analysis-suitable T-splines can be locally refined (Scott et al., 2010) and provide a partition of unity (Li et al., 2010).

The results in this paper suggest several interesting problems for future research. For T-splines that do have V2-subgraphs, linear independence is

ascertained by assessing the nullity of the column-reduced matrix M. The nullity of M can be expressed as a system of rational polynomial equations whose members are minors of the column-reduced M and whose variables are knots. What is the dimension of the solution set of such systems of equations? For example, we conjecture that no T-mesh topology exists that is linearly dependent for all knot vectors. The only examples of linearly dependent T-splines that we are aware of have multiple knots. Do there exist examples of linearly dependent T-splines for which there are no multiple knots?

Another topic for future research is to devise a version of analysis-suitable T-splines for arbitrary topology (i.e., for which extraordinary points are allowed in the control grid) that assures linear independence.

Acknowledgements

This work was supported by the Office of Naval Research ONR Grant Numbers NOOO14-08-C-0920 and N00014-08-1-0992, and by the ARC 9/09 Grant (MOE2008-T2-1-075) of Singapore.

References

Bazilevs, Y., Calo, V.M., Cottrell, J.A., Evans, J.A., Hughes, T.J.R., Lipton, S., Scott, M.A., Sederberg, T.W., 2010. Isogeometric analysis using T-splines. Computer Methods in Applied Mechanics and Engineering 199, 229 – 263.

Buffa, A., Cho, D., Sangalli, G., 2010. Linear independence of the T-spline blending functions associated with some particular T-meshes. Computer Methods in Applied Mechanics and Engineering 199, 1437 – 1445.

Cottrell, J., Hughes, T.J.R., Bazilevs, Y., 2009. Isogeometric Analysis: Toward Integration of CAD and FEA. John Wiley & Sons, Ltd.

Finnigan, G.T., 2008. Arbitrary Degree T-splines. Master's thesis. Brigham Young University, Department of Computer Science.

Li, X., Zheng, J., Sederberg, T.W., 2010. On T-spline classification. In preparation .

Scott, M.A., Hughes, T.J.R., Li, X., Sederberg, T.W., 2010. Local refinement of standard T-meshes. In preparation .

Sederberg, T.W., Cardon, D.L., Finnigan, G.T., North, N.S., Zheng, J., Lyche, T., 2004. T-spline simplification and local refinement. ACM Trans. Graph. 23, 276–283.

Sederberg, T.W., Finnigan, G.T., Li, X., Lin, H., Ipson, H., 2008. Watertight trimmed NURBS. ACM Trans. Graph. 27, 1–8.

Sederberg, T.W., Zheng, J., Bakenov, A., Nasri, A., 2003. T-Splines and T-NURCCs. ACM Transactions on Graphics 22, 477–484.